PHYSICAL REVIEW B **74**, 140410(R) (2006)

# $^{55}$Mn NMR investigation of the correlation between antiferromagnetism and ferroelectricity in $TbMn_2O_5$

S.-H. Baek, A. P. Reyes, M. J. R. Hoch, W. G. Moulton, P. L. Kuhns, and A. G. Harter
*National High Magnetic Field Laboratory, Tallahassee, Florida 32310, USA*

N. Hur and S.-W. Cheong
*Department of Physics and Astronomy, Rutgers University, Pistacaway, New Jersey 08854, USA*
(Received 16 October 2006; published 31 October 2006)

The correlation between antiferromagnetism and ferroelectricity in magnetoelectric multiferroic $TbMn_2O_5$ has been investigated by zero-field $^{55}$Mn NMR. Antiferromagnetic transition near 40 K is found to be first order. When an external field up to 7 T is applied along the easy *a* axis, a dramatic change in the signal intensity is observed which is hysteretic in nature. Such effects are absent for *H* along the *b* and *c* axes. The observed field-induced signal enhancement is attributed to antiferromagnetic domain walls which are strongly coupled to ferroelectric domain walls. Experimental data suggest that this may be related to the field-induced ferromagnetic ordering of the Tb ion.

DOI: 10.1103/PhysRevB.74.140410 PACS number(s): 76.60.−k, 75.80.+q, 75.60.Ch, 77.80.−e

The $RMn_2O_5$ family ($R$=Y, Bi, Rare earth) is one of the class of materials known as multiferroics which exhibit simultaneous ferroelectric (FE) and antiferromagnetic (AFM) order. They have a complex structure (orthorhombic, space group *Pbam*) involving infinite chains of $Mn^{4+}O_6$ octahedra along the *c* axis which are interconnected by $Mn^{3+}O_5$ square pyramids and $RO_8$ units.[1,2] Among the $RMn_2O_5$ family, $TbMn_2O_5$ shows a unique magnetoelectric effect thought to be due to the large magnetic moment and the large magnetic anisotropy of the $Tb^{3+}$ ion. The magnetic structure has been investigated by a number of groups using neutron diffraction techniques.[1,3,4] This work together with magnetic and dielectric studies[5,6] has shown that the electric polarization ($P$) and dielectric constant ($\epsilon$) undergo four transitions associated with anomalies in the magnetic susceptibility ($\chi$). As the temperature ($T$) is lowered, incommensurate AFM ordering of Mn spins occurs at $T_N$=43 K followed by the onset of ferroelectricity at 38 K, a transition to a commensurate phase at 33 K, corresponding to a maximum in $P$, and a transition back to an incommensurate phase at 24 K where $\epsilon$ increases significantly. At around 10 K $\chi$ increases and this is attributed to magnetic ordering involving the Tb moments.

The recent experiments of Hur *et al.*[5] showed that $P$ can be completely reversed at 3 K by applying a magnetic field $H$ in the range 0–2 T along the crystal *a* axis. They proposed a model involving two oppositely directed electric dipole moments, one of which is sensitive to $H$. The present $^{55}$Mn NMR experiments have been performed in an effort to gain microscopic understanding of the processes involved in this polarization switching effect.

The experiments were carried out on a single crystal ($2\times3\times4$ mm$^3$) of $TbMn_2O_5$, which was grown as described in Ref. 3. The $^{55}$Mn spectra were obtained by integrating averaged spin echo signals as the frequency was swept through the resonance line. We used a coherent pulsed NMR spectrometer capable of computer-controlled tuning of a probe that was calibrated over the whole frequency range. Because of strong ferromagnetic (FM) behavior at low-$T$, we observed a considerable tendency of the crystal to reorient the *a* axis parallel to $H$ when a perturbing field is applied. The crystal was mounted in a clamp to prevent reorientation. The axis of the NMR coil was oriented along the crystal *c* axis.

Figure 1 shows zero-field (ZF) NMR spectra obtained at 1.8 K under three different conditions: (i) cooling at zero field (ZFC), (ii) following ZFC, applying $H$=7 T and removing it, and (iii) field-cooling (FC) in $H$=3 T parallel to the crystal *a* axis. The spectra consist of three main components, a fairly sharp main peak at 265 MHz and two secondary peaks at 250 and 258 MHz. We attribute the NMR signal to AFM coupling of $Mn^{3+}$ ions ($\gamma$=10.5 MHz/T) inducing a hyperfine field $H_{hf}\sim25$ T. This is supported by the fact that the signal appears only below 40 K where the Mn ions order.

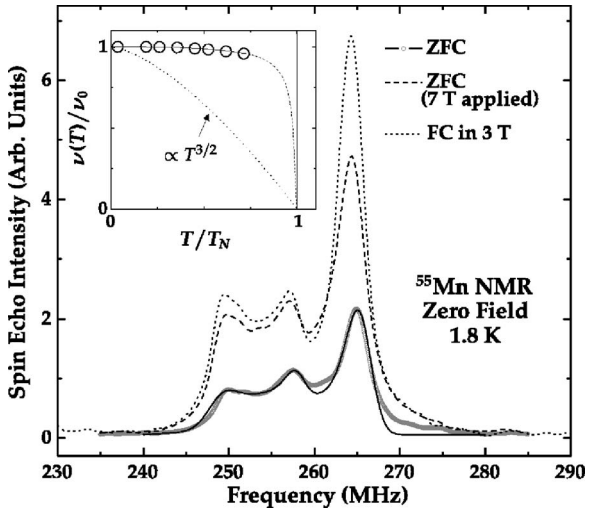


FIG. 1. Zero-field $^{55}$Mn NMR spectrum of $TbMn_2O_5$ at 1.8 K following three different cooling procedures (see text). The solid line was obtained using Eq. (1) with appropriate choice of parameters. Inset: Reduced sublattice magnetization deduced by tracking the resonance frequency at the main peak up to 33 K. Dotted line shows conventional $T^{3/2}$ behavior.

 

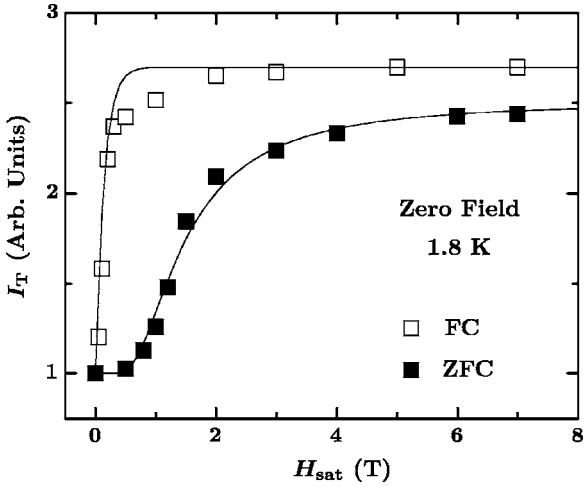


FIG. 2. Integrated signal intensity $I_T$ vs $H$ at 1.8 K following FC and ZFC obtained at zero field after removal of $H_{sat}$. Solid lines are guides to eyes.

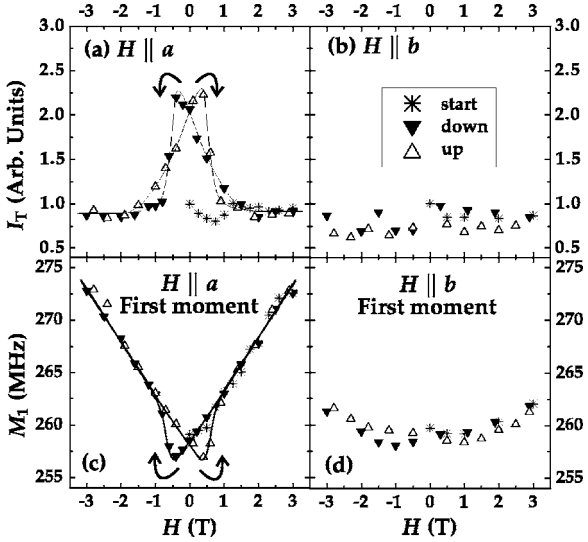


FIG. 3. $^{55}Mn^{3+}$ NMR signal intensity vs $H$ at 1.8 K following ZFC (a) $H\|a$ and (b) $H\|b$. The lower two panels (c) and (d) show the first moment of the spectrum. A field of up to ±7 T was applied before the direction of $H$ was reversed.

While the equilibrium spectral shape and frequency distribution are insensitive to $T$ it is found that the signal amplitude depends on the magnetic history, as evident in Fig. 1. The temperature dependence of the resonance frequency of the largest peak is shown in the inset of Fig. 1. The signal is observed up to 33 K but becomes very weak above this temperature.

Remarkably, the signal amplitude is largest after the sample is cooled in $H>2$ T. This can be seen in Fig. 2 where the total signal intensity ($I_T$) *at zero field* is plotted against a saturation field $H_{sat}$. For the FC case, $H_{sat}$ is the immersion field, while for ZFC, $H_{sat}$ is applied and then removed after the sample has cooled down. The maximum $I_T$ is larger for the FC case, giving a signal enhancement of ~2.7, achieved at $H_{sat}\sim 2$ T. In the ZFC case $I_T$ shows a gradual increase with $H_{sat}$ and has not reached a plateau for $H$ as high as 7 T. The signal enhancement is observed up to 25 K. The enhancement of intensity is reminiscent of a similar effect in FM systems, where very large enhancements are generally found. Below 25 K the Tb moments order ferromagnetically[3,5] for $H\sim 2.5$ T and it is likely that the ZF signal enhancements after FC or ZFC followed by cycling of $H$, as shown in Fig. 2, are linked to this ordering. The enhancement mechanism involves rf coupling to the hyperfine field at the $Mn^{3+}$ sites.[7]

The variation of the total signal intensity $I_T$ is shown in Figs. 3(a) and 3(b) for $H\|a$ and $H\|b$, respectively. Figures 3(c) and 3(d) show the first moment (or centroid frequency, $M_1$) of the spectrum as a function of $H$, revealing a large anisotropy in the system. For $H\|a$, we find (i) an initial small irreversible decrease in $I_T$ from 0 to 1 T following the first application of $H$, (ii) small hysteresis effects on reversing $H$ after field cycling, (iii) a sudden drop of $I_T$ at ~±0.5 T accompanied by the change of $M_1$, and (iv) a complete hysteresis loop in the range ~±2 T. With regard to the last point, it is interesting to note that 2 T corresponds to the field at which field-induced FM ordering of Tb occurs.[3] In the case of $H\|b$, $I_T$ does not change and very small hysteresis in $M_1$ is observed as shown in Figs. 3(b) and 3(d). We note that the spectral peaks did not split as expected for a conventional antiferromagnet in an applied field. This suggests that the signal comes from sample regions such as domain walls in which some shielding mechanism operates.

If $H$ is not reversed, we observed that $I_T$ and $M_1$ are *completely reversible and track H*. This behavior is depicted in Fig. 4, where $H$ is cycled only in the positive direction. This is the exact magnetic analogue of the polarization reversal observed by Hur *et al.*[5]

Before attempting to account for these observations we briefly comment on the observed NMR spectrum. The magnetic moments associated with the $Mn^{3+}$ ($4h$ site, $t_{2g}^3 e_g^1$) and $Mn^{4+}$ ($4f$ site, $t_{2g}^3$) ions were reported to be 2.4 $\mu_B$ and 1.81 $\mu_B$, respectively at 27 K.[3] Since the dominant contribution to the hyperfine field arises from the core polarization term, the maximum $H_{hf}$ values at nuclear sites are estimated

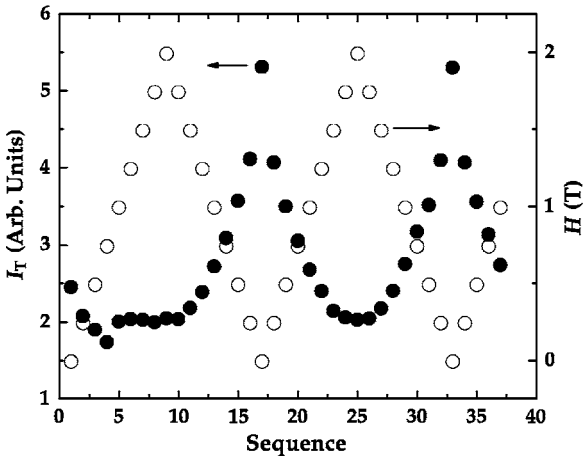


FIG. 4. $^{55}Mn$ NMR signal intensity (closed circles) of $TbMn_2O_5$ at 1.8 K as a function of applied field (open circles) in the range 0–2 T. The signal intensity changes reversibly with applied field.

to be $-12.13\ \mathrm{T}/\mu_B$ for $Mn^{3+}$ and $-9.76\ \mathrm{T}/\mu_B$ for $Mn^{4+}$.[8] Using these values we expect to observe $Mn^{3+}$ and $Mn^{4+}$ NMR lines at ~306 and ~185 MHz, respectively. On this basis, we assign the 240–280 MHz line to the $Mn^{3+}$ ions. The observed resonance frequency is slightly less than the estimated value for $Mn^{3+}$ but one that is reasonably expected if we take into account small isotropic transferred hyperfine fields from adjacent ions which have the opposite sign and thus reduce the coupling.

The normalized sublattice magnetization obtained by tracking the reduced resonance frequency $\nu(T)/\nu(0)$ for the main peak, which is expected to vanish as $T \to T_N$, is shown in the inset of Fig. 1. The values decrease only slightly over the temperature range for which measurements could be made, and cannot be fit to molecular field theory even qualitatively. This implies that the transition at $T_N$ is of first order. In comparison we show the Bloch $T^{3/2}$ law (dotted line) curve in conventional magnets.

Next we discuss the origin of the structure of the spectrum. First, we consider the possibility of a single magnetic site with large quadrupole coupling $\nu_Q$ and anisotropy parameter $\eta \to 1$. Lattice sum calculations of the electric field gradient (EFG) show that $\eta \sim 0.88$ (in agreement with Mössbauer results[9] for $YMn_{1.97}Fe_{0.03}O_5$) with the EFG principal axis at 14° with respect to the $a$ axis. However, the quadrupole coupling required for this fit is ~40 MHz, which is much larger than expected for Mn ions.

A second possibility is that the three peaks come from four overlapping magnetically non-equivalent sites having $\nu_Q \ll$ linewidth, $\Delta f$. This is implied in the neutron data, which[1,3] show that at temperatures between 1.5 and 27 K both $Mn^{4+}$ and $Mn^{3+}$ moments lie in the $ab$ plane with each type of ion canted at 10° and 24° from the $a$ axis.[3] The sublattice magnetization further differentiates each site. The measured spin-lattice relaxation times $T_1$ for the two major spectral components differ by a factor of 10 and this justifies their assignments to different crystallographic sites. This is consistent with Mössbauer results[9] for the structurally similar material $YMn_{1.97}Fe_{0.03}O_5$ in which the $Mn^{3+}$ sites form two sublattices with the $H_{\mathrm{hf}}$ vectors perpendicular to each other. Although these two models can reproduce the observed spectra, the anomalous behavior of signal intensity presents a complication.

In the light of the hysteretic nature of the signal intensity, it is appealing to consider a third possibility where the NMR signal that we observe arises from domain walls. This is discussed in detail below. In this case, one can model the spin structure as helical order in which $H_{\mathrm{hf}}$ may or may not be commensurate with the lattice. An anisotropic hyperfine field distribution can produce the same spectral shape as helical order. We adopt the theoretical model developed for a spatially spin-modulated structure following Ref. 10. The lineshape can be modeled with a Gaussian broadening function by

$$P(\nu) \propto \int_0^{\pi} (m^{-1} - 1 + \sin^2\theta)^{-1/2} (\Delta_{\parallel} + \delta_l \sin^2\theta)^{-1} \times \exp\left\{ - \frac{2[\nu - (\nu_{\parallel} - \delta\nu \sin^2\theta)]^2}{(\Delta_{\parallel} + \delta_l \sin^2\theta)^2} \right\} d\theta, \quad (1)$$

where $m$ is an adjustable parameter determining the asymmetric character of the spectrum (i.e., the lineshape becomes asymmetric with $m \to 1$ and symmetric with $m \to 0$), $\Delta$ the local linewidth, and $\nu$ the local frequency, with

$$\nu(\theta) = \nu_{\parallel} - (\nu_{\parallel} - \nu_{\perp})\sin^2\theta = \nu_{\parallel} - \delta\nu \sin^2\theta, \quad (2)$$

$$\Delta(\theta) = \Delta_{\parallel} + \delta_l \sin^2\theta. \quad (3)$$

The subscripts $\parallel$ and $\perp$ represent $\mathbf{L} \parallel a(\theta = 0)$ and $\mathbf{L} \perp a(\theta = \pi/2)$, respectively, with $\mathbf{L}$ the antiferromagnetic vector, $\Delta_{\parallel}$ is the minimum linewidth at $\nu_{\parallel}$, and $\delta_l$ is the additional broadening at $\nu_{\perp}$. Equation (1) predicts two peaks with the larger peak on the high frequency side. To fit the spectrum in Fig. 1 it is necessary to assume two different sets of spin structures with different values of the parameters. It turns out that $m$ is the most sensitive parameter and choosing $\nu_{\parallel}$ and $\nu_{\perp}$ is somewhat arbitrary. The choice of parameters $m \sim 0.9$, $\Delta_{\parallel} = 2.5$ MHz, and $\delta_l = 0.1\Delta_{\parallel}$ gives a satisfactory fit to the experimental data as shown by the solid line in Fig. 1.

We now discuss the possible origin of the observed hysteresis in the signal intensity in terms of domains and domain walls in the AFM lattice. As mentioned earlier, it is well known that in FM material the ZF NMR signal is strongly enhanced by a factor $\eta_E \sim 10^3 - 10^5$ for nuclei in domain walls. When external fields are applied, the domain walls are swept out and the enhancement is drastically reduced. In the case of AFM system, the existence of domain walls is not very well studied. However, it is possible for a multidomain structure to form if there are lattice imperfections.[11,12] Indeed AFM domain structure have been observed in a number of systems, e.g., $\alpha$-$Fe_2O_3$, UPdSn, and Cr.[13–15] In particular, $^{57}$Fe NMR studies on $\alpha$-$Fe_2O_3$ (hematite) reveal hysteresis effects in the signal intensity attributed to AFM domain wall enhancement.[16,17] Similar behavior is found in CuMn by ZF $^{63,65}$Cu NMR.[18] In the spin-glass CuMn, the signal enhancements are ascribed to domain rotation by the rf field, in which the otherwise absent domain structure is induced by $H$. In $RMn_2O_5$, the structural distortion that gives rise to the ferroelectricity may favor the formation of AFM domains. While there is no direct evidence of AFM domain walls in $TbMn_2O_5$, recent work has suggested that strained FE and 180° AFM domain walls are clamped together in the hexagonal manganites $YMnO_3$ and $HoMnO_3$.[19–22]

In the AFM domain wall model suggested in Ref. 11, there are two types of domain walls: movable or free walls (which can exist even in perfect crystals) and pinned or clamped walls. The fact that $I_{\mathrm{T}}$ decreases initially with $H$ [Fig. 3(a)] is consistent with movable walls being swept out. With increasing $H$ it is likely that at least some of the AFM walls are clamped at FE walls. The AFM walls and FE walls remain locked in place unless $T$ is raised above a critical temperature.[20] This model explains the irreversible change of the signal enhancement after first application of $H$ as shown in Fig. 3(a) and the fact that this effect is reinitialized only when $T$ is raised above $T_N \sim 43$ K and then lowered again. It has been suggested that the coupling between AFM walls and FE walls is very strong and the sign of the product of the AFM and the FE order parameters is maintained.[19] In this scenario of direct coupling between the two walls, the absence of NMR enhancement effects for $H \parallel b$ [see Fig. 3(b)] is

linked to the strong uniaxial ferroelectricity along the *b* axis.[5] With regard to the lineshape, Eq. (1) is applicable in this domain wall model if we assume an isotropic distribution of the spins in the domain walls.

What is the role of Tb in the multiferroicity of $TbMn_2O_5$? Chapon *et al.*[3] have suggested that the *H*-induced ordering of the Tb moments is responsible for reversible polarization in this compound. This interpretation correlates with the observed reversible NMR signal enhancement in Fig. 4. Moreover, the fact that the enhancement saturates at 2 T correlates well with the saturation of magnetization due to Tb moments. And, finally, it was recently shown that the FM ordering of Tb can be induced up to 25 K,[23] where the signal enhancement is also observed. While direct evidence of the role of Tb is not available from NMR, these correlations suggest that Tb ordering is important in determining the low-*T* properties of the material.

In summary, $^{55}Mn$ NMR provides a probe of the $Mn^{3+}$ ion's magnetic environment in $TbMn_2O_5$. The information obtained from the field-induced changes in the signal enhancement factor is consistent with the Tb moments playing a role in determining the interesting magnetoelectric properties of this material. The reversible shift of the centroid for *H* along the *a* axis in the range 0–2 T is attributed to changes in the transferred hyperfine coupling at $Mn^{3+}$ sites induced by the Tb ordering. Small displacement of the $Mn^{3+}$ ions involved in the field-induced electric polarization produces changes in the transferred hyperfine coupling from other magnetic ions. The signal enhancement, observed in the same range of applied magnetic fields provides evidence that domain structures are important in $TbMn_2O_5$ with NMR signals coming largely from domain wall regions. Relaxation experiments and experiments in magnetically inert $YMn_2O_5$ are currently underway.

We thank R. Guertin, R. Smith, and R. Achey for experimental assistance, and K. H. Kim for useful discussion and sharing valuable phase diagram data. This work was supported by NSF in-house research program State of Florida under cooperative agreement DMR-0084173. Work at Rutgers was supported by the NSF-DMR-0520471.

[1] G. Blake, L. Chapon, P. Radaelli, S. Park, N. Hur, S.-W. Cheong, and J. Rodríguez-Carvajal, Phys. Rev. B **71**, 214402 (2005).
[2] J. Alonso, M. Casais, M. Martinez-Lope, J. Martines, and M. Fernández-Diaz, J. Phys.: Condens. Matter **9**, 8515 (1997).
[3] L. Chapon, G. Blake, M. Gutmann, S. Park, N. Hur, P. Radaelli, and S.-W. Cheong, Phys. Rev. Lett. **93**, 177402 (2004).
[4] P. Gardner, C. Wilkinson, J. Forsyth, and B. Wanklyn, J. Phys. C **21**, 5633 (1988).
[5] N. Hur, S. Park, P. Sharma, J. Ahn, S. Guha, and S.-W. Cheong, Nature (London) **429**, 392 (2004).
[6] K. Saito and K. Kohn, J. Phys.: Condens. Matter **7**, 2855 (1995).
[7] E. Turov and M. Petrov, *Nuclear Magnetic Resonance in Ferro- and Antiferromagnets* (Halsted Press, New York, 1972).
[8] A. Freeman and R. Watson, in *Magnetism IIA*, edited by G. Rado and H. Suhl (Academic, New York, 1965).
[9] I. Kagomiya, S. Nakamura, S. Matsumoto, M. Tanaka, and K. Kohn, J. Phys. Soc. Jpn. **74**, 450 (2005).
[10] A. Zalesskiĭ, A. Frolov, A. Zvezdin, A. Gippius, E. Morozova, D. Khozeev, A. Bush, and V. Pokatilov, J. Exp. Theor. Phys. **95**, 101 (2002).
[11] Y.-Y. Li, Phys. Rev. **101**, 1450 (1956).
[12] T. Yamada, J. Phys. Soc. Jpn. **21**, 650 (1966).
[13] I. Maartense and C. Searle, J. Appl. Phys. **42**, 2349 (1971).
[14] H. Nakotte, R. Robinson, A. Purwanto, Z. Tun, K. Prokes, E. Brück, and F. de Boer, Phys. Rev. B **58**, 9269 (1998).
[15] P. Evans, E. Isaacs, G. Aeppli, Z. Cai, and B. Lai, Science **295**, 1042 (2002).
[16] D. Anderson, Phys. Rev. **151**, 247 (1966).
[17] A. Hirai, J. Eaton, and C. Searle, Phys. Rev. B **3**, 68 (1971).
[18] H. Alloul, Phys. Rev. Lett. **42**, 603 (1979).
[19] M. Fiebig, T. Lottermoser, D. Fröhlich, A. Goltsev, and R. Pisarev, Nature (London) **419**, 818 (2002).
[20] A. Goltsev, R. Pisarev, T. Lottermoser, and M. Fiebig, Phys. Rev. Lett. **90**, 177204 (2003).
[21] T. Lottermoser and M. Fiebig, Phys. Rev. B **70**, 220407(R) (2004).
[22] B. Lorenz, A. Litvinchuk, M. Gospodinov, and C. Chu, Phys. Rev. Lett. **92**, 087204 (2004).
[23] K. H. Kim (private communication).